Sensorless Vector Controlled Induction Machine in Field Weakening Region: Comparing MRAS and ANN-Based Speed Estimators

Samir Moulahoum* and Omar Touhami**

Abstract – The accuracy of all the schemes that belong to vector controlled induction machine drives is strongly affected by parameter variations. The aim of this paper is to examine iron losses and magnetic saturation effect in sensorless vector control of induction machines. At first, an approach to induction machine modelling and vector control scheme, which account for both iron loss and saturation, is presented. Then, a model reference adaptive system (MRAS) based speed estimator is developed. The speed estimation is modified in such a way that iron losses and the variation in the saturation level are compensated. Thus by substituting an artificial neural network flux estimator into the MRAS speed estimator. Experimental results are presented to verify the effectiveness of the proposed approach.

Keywords: ANN, Induction Machine, Iron Loss, MRAS, Sensorless Vector Control, Saturation.

1. Introduction

The conventional linear modelling of induction machines fails to deliver accurate results and makes performance predictions almost impossible in a number of operating conditions [1], the saturation effect has been suspected as the prime cause of detuning. Several modeling techniques have been proposed in the literature, based mainly on modifications of the equivalent circuit and the d-q model, including mutual dependence on the flux or magnetizing currents. The 'cross saturation' model has become the standard method of accounting for these effects [2].

Another area of improvement has been the incorporation of iron loss effect in induction modeling. Nowadays, more induction motors are fed by PWM inverters. The use of static converter for electrical drives leads to iron loss increase [3]. Different models have been developed; the approach used, in general, to include iron loss in the induction machine model is connecting R_{Fe} in parallel with the magnetizing branch [3-4]. However, it was shown in [5] that by appropriate modification, an equivalent iron loss resistance can be placed in series to the mutual inductance.

The vector control drive requires the induction motor speed as a feedback signal; a rotational encoder is used to obtain this speed, which degrades the system reliability, especially in hostile environments. Sensorless vector control is proposed to cope with the speed sensing problem. Various approaches of sensorless vector control have been presented in the literature.

In this paper, first of all, a model, based on a nonlinear circuit of the machine, that simultaneously includes both magnetic saturation and iron loss is presented. A vector control modified scheme is used that is insensitive to the saturation effect as well as to iron losses.

Then, we propose a MRAS speed estimation which is based on an e.m.f measurement instead of stator voltage measurement. A modified integration method is used to avoid the offset problem caused by open loop integration in the reference model [6]. In the flux weakening operation, the saturation level changes; however, a MRAS speed estimator uses a constant value of magnetizing inductance, which leads to error between the real speed and the estimated speed. Levi et al [7] propose a modified speed estimator that takes into account and compensates saturation effect. In this paper, we propose, with the same goal but differently, an artificial neural network that is used to modify the estimated rotor flux. The ANN flux estimator is substituted into the MRAS speed estimator to improve the performance of the rotor speed estimation, particularly, in the flux weakening region. The estimated speed replaces the feedback signal for vector control and speed control. The ANN is trained on line with the backpropagation training method. In order to overcome the slow convergence of the training method, the modification of rotor flux estimation presented in [8] is exploited.

The performance of the proposed estimators are compared and discussed for nominal operation. Its limits are also addressed in a low speed range. The improvements achieved at flux weakening operation with the ANN- based

* Dept. of Electrical Engineering, Yahia Farès University, Médéa, Algeria (Samir.Moulahoum@green.uhp-nancy.fr)

** Electrotechnical Research Laboratory, National Polytechnic School, Algiers, Algeria. (omar.touhami@enp.edu.dz)

Received 30 June, 2006 ; Accepted 16 March, 2007

speed estimator are outlined and discussed.

2. Vector Controlled Induction Machine

2.1 Induction Machine Modeling

The treatment of saturation has been considered in detail by a number of authors, and numerous methods with a varying level of complexity are available. In this paper, the saturation effect in induction machines is associated with the magnetizing flux. Including saturation in d-q axis model consists in expressing the flux linkages and their time derivatives as a function of currents. This dependence may be determined from a no-load test carried out on the machine. However, saturation and iron losses occur simultaneously. Hence, in the proposed model, the principles of magnetizing flux saturation modelling and derivation procedure remain the same as for an induction machine without iron loss. However, the overall complexity of the model increases when the iron losses branch is added (Fig.1). As consequence the number of differential equations increases. Details of induction machine modelling process by considering iron loss and saturation can be found in [4]. The model can be formed in various different ways, depending on the set of state-space variables. The model selected is the one with current components as state-space variables. It may be given in a matrix form as:

$$[V]=[L][\dot{i}]+[R][I] \tag{1}$$

with $$[I]=[I_{ds} \quad I_{qs} \quad I_{dr} \quad I_{qr} \quad I_{dFe} \quad I_{qFe}]^T$$

$$[V]=[V_{ds} \quad V_{qs} \quad 0 \quad 0 \quad 0 \quad 0]^T$$

$$[L]=\begin{bmatrix} L_{\sigma s}+M_d & M_{dq} & M_d & M_{dq} & -M_d & -M_{dq} \\ M_{dq} & L_{\sigma s}+M_q & M_{dq} & M_q & -M_{dq} & -M_q \\ M_d & M_{dq} & L_{\sigma r}+M_d & M_{dq} & -M_d & -M_{dq} \\ M_{dq} & M_q & M_{dq} & L_{\sigma r}+M_q & -M_{dq} & -M_q \\ -M_d & -M_{dq} & -M_d & -M_{dq} & M_d & M_{dq} \\ -M_{dq} & -M_q & -M_{dq} & -M_q & M_{dq} & M_q \end{bmatrix}$$

$$[R]=\begin{bmatrix} R_s & -\omega_s L_s & 0 & -\omega_s L_m & 0 & \omega_s L_m \\ \omega_s L_s & R_s & \omega_s L_m & 0 & -\omega_s L_m & 0 \\ 0 & -\omega_{sl} L_m & R_r & -\omega_{sl} L_r & 0 & \omega_{sl} L_m \\ \omega_{sl} L_m & 0 & \omega_{sl} L_r & R_r & -\omega_{sl} L_m & 0 \\ 0 & \omega_s L_m & 0 & \omega_s L_m & R_{Fe} & -\omega_s L_m \\ -\omega_s L_m & 0 & -\omega_s L_m & 0 & \omega_s L_m & R_{Fe} \end{bmatrix}$$

Where M_d and M_q are, respectively, the d and q mutual inductances. M_{dq} is the term that handles the "saturation cross effect". The magnetizing curve and equivalent iron loss resistance have to be known, these are determined by a standard no-load test on an induction machine.

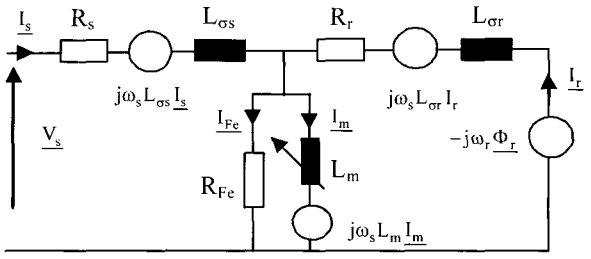

Fig. 1. The equivalent circuit of an induction machine considering iron losses and magnetic saturation

2.2 Vector Controller Scheme

Neglecting iron loss and saturation effect in vector controller causes a coupling between flux and torque and hence the torque in the machine will be lower than the reference one. Therefore, modifying the basic vector control scheme may be necessary. Derivation of the modified vector controller is obtained by a modification of Fig. 1. The non linear function $L_m(\Phi_m)$ is used to include the saturation effect in the controller model. Details of the modified vector controller that takes into account magnetic saturation and iron loss can be found in [9-10].

The complete modified vector controller that is based on stator currents and rotor speed measurements, which takes into account saturation and iron losses, can be given by the following system:

$$\begin{aligned} &\Phi_{dm}^* = \Phi_r^* \qquad \Phi_m^* = \sqrt{\Phi_{dm}^{*2} + \Phi_{qm}^{*2}} \\ &\Phi_{qm}^* = \frac{L_{\sigma r} T_{em}^*}{P \Phi_r^*} \qquad \omega_{sl}^* = \frac{(L_m^* - T_{Fr}^* R_{Fr}^*) I_{qs}^*}{T_{Fr}^* \Phi_r^*} \\ &I_{qs}^* = \frac{T_{em}^* L_r^*}{P L_m^* \Phi_r^*} \qquad I_{ds}^* = \frac{\Phi_r^*}{(L_m^* - R_{Fr}^* T_{Fr}^*)} \\ &L_m^* = L_m^*(\Phi_m^*) \qquad \omega_s^* = \omega_{sl}^* + \omega_r \\ &V_{ds}^* = V_{dsl}^* - \sigma L_s^* \omega_s^* I_{qs}^* + \frac{R_{Fs}^*}{L_r^*} \Phi_r^* \\ &V_{qs}^* = V_{qsl}^* + \omega_s^* (\sigma L_s^* I_{ds}^* + \frac{L_m^*}{L_r^*} \Phi_r^*) \end{aligned} \tag{2}$$

* indicates reference values. V_{dsl}^* and V_{qsl}^* are current controllers' outputs and:

$$R_{Fs}^* = \frac{\omega_s^{*2} L_m^{*2}}{R_{Fe}} \qquad R_{Fr}^* = \frac{\omega_{sl}^* \omega_s^* L_m^{*2}}{R_{Fe}} \qquad T_{Fr}^* = \frac{L_r^*}{R_{Fr}^* + R_r}$$

The bloc diagram of this controller is shown in Fig. 2.

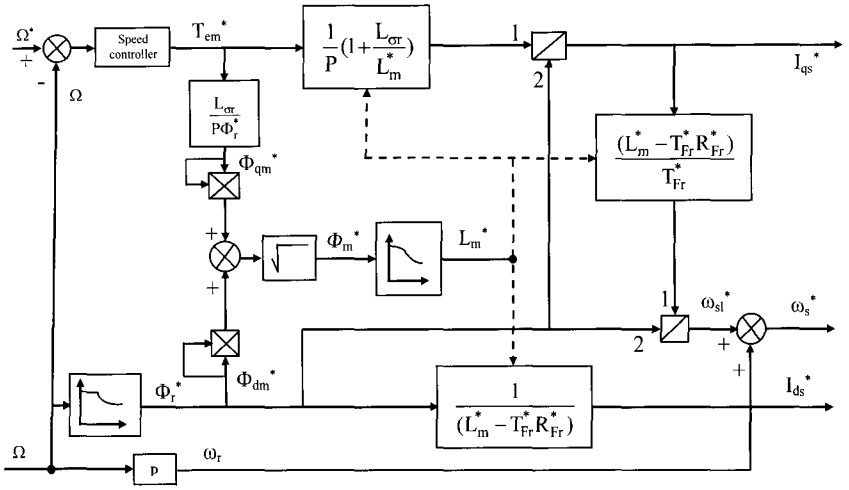

Fig. 2. Modified vector controller of an induction machine with iron losses and saturation compensation

3. Sensorless Drive Scheme

As shown in [10], the proposed vector controller gives high torque and speed control performances and interesting dynamic responses. However, this type of controller requires a mechanical sensor which needs extra mounting arrangements on the shaft of the motor, thus reducing its reliability as well as increasing the overall cost of the drive and constitutes a fragile part of the plant. To eliminate the use of this sensor, several algorithms have been proposed to estimate speed. This section deals with a model reference adaptive system (MRAS) speed estimator and an artificial neural network (ANN)-based MRAS speed estimator. Performances of sensorless vector control associated to these speed estimators are analyzed. The effect of saturation and iron losses in flux weakening operation is examined and compensated.

The major problem in the practical implementation of the speed estimator is the presence of an offset in the pure integration of flux estimation. This offset, be it as little as it is, affects the accuracy of the flux estimation and leads to the loss of system control if not handled. Several methods have been used to solve this problem, some authors substitute the integration by a low-pass filtering [7-11], others use an adaptive filter [8]. The method used here to eliminate the offset is proposed in [6]. In the machine used in the experimental setup, extra small holes were designed along the stator core. They contain two orthogonal windings which give images of α and β e.m.f. The two signals are measured, their amplitudes are adjusted and the offsets are eliminated from the signals using an on line offset tracking scheme. In steady state operation, α and β stator flux are sinusoidal but their mean value is not null depending on the offset of their corresponding e.m.f, knowing that when one of the two flux signals is maximum or minimum the other must be null. Hence, at each extreme, we eliminate the corresponding offset of the other flux variable. Fig. 3 shows the experimental α and β stator flux when offsets are auto-tuned.

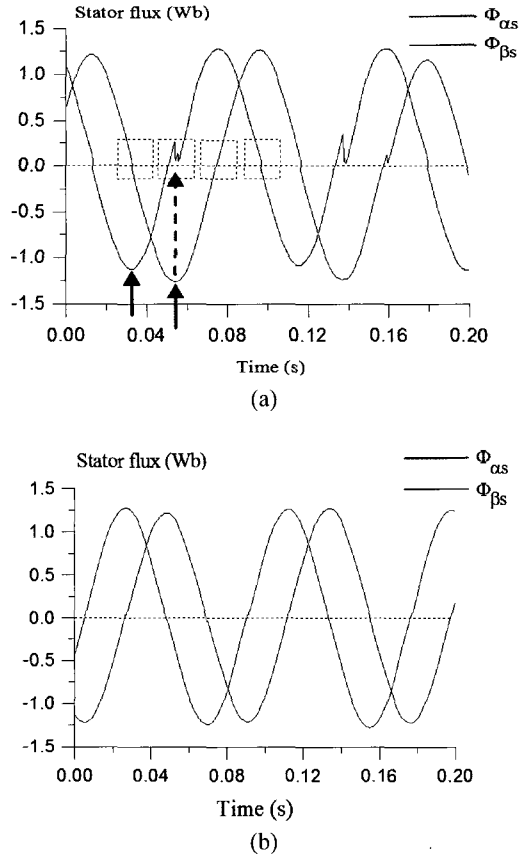

Fig. 3. The stator flux estimation with the offset compensation algorithm
(a) The stator flux while offsets are not tuned
(b) The stator flux after compensated offsets

3.1 MRAS Speed Estimator

In the MRAS speed estimator, the reference model is based on the well-known stator equations written in the stationary reference frame (voltage model indexed by '1'), while the adjustable model is derived from the rotor equations in the same reference frame (current model indexed by '2') [12]. In the MRAS exposed in this paper, the measured E.M.F is used instead of the E.M.F reconstituted from stator voltage and resistive voltage drop. So, this scheme does not need a stator resistance value; as a consequence, variations of this resistance have essentially no impact on the speed estimation.

By introducing the E.M.Fs, the classical MRAS speed estimator is described by:

$$\frac{d\Phi_{(\alpha,\beta)r1}}{dt} = \frac{L_m}{L_r}\left(E_{(\alpha,\beta)s} - \sigma L_s \frac{dI_{(\alpha,\beta)s}}{dt}\right) \quad (3)$$

$$\frac{d\Phi_{(\alpha,\beta)r2}}{dt} = (j\omega_r - \frac{1}{T_r})\Phi_{(\alpha,\beta)r2} + \frac{L_m}{T_r} I_{(\alpha,\beta)s} \quad (4)$$

$$\varepsilon = \Phi_{\alpha r2}\,\Phi_{\beta r1} - \Phi_{\alpha r1}\,\Phi_{\beta r2} \quad (5)$$

The error ε is brought to zero by a PI controller. The output of this controller is the estimated speed. The MRAS estimator is shown in Fig. 4. The offset voltage compensation is introduced in the speed estimator but not shown in the figure.

3.2 ANN speed estimator

The most commonly used neural networks are feedforward multilayer networks where no information is fed back during application. Most often, the backpropagation training is used to adjust the neural network weights, since the training algorithm takes a long time to converge. Two layered neural networks are, therefore, preferred. This type of neural network may learn on-line, so, the off-line training is not necessary. To use artificial neural network (ANN) in speed estimation, the voltage and current models in the stationary reference frame are necessary. The voltage model is used as a reference model, and the current model is considered as an ANN adjustable model. The output of the ANN is defined as the estimated speed. The flux error is backpropagated to the ANN and the weights are adjusted on line to reduce error. Finally, the output of the ANN follows the real speed. The adjustable model can be transformed into the followings numerical form using the backward difference method:

$$\begin{bmatrix}\Phi_{\alpha r2}[k]\\ \Phi_{\beta r2}[k]\end{bmatrix} = \begin{bmatrix}w_1\Phi_{\alpha r1}[k-1] - w_2\Phi_{\beta r1}[k-1] + w_3 I_{\alpha s}[k-1]\\ w_1\Phi_{\beta r1}[k-1] + w_2\Phi_{\alpha r1}[k-1] + w_3 I_{\beta s}[k-1]\end{bmatrix} \quad (6)$$

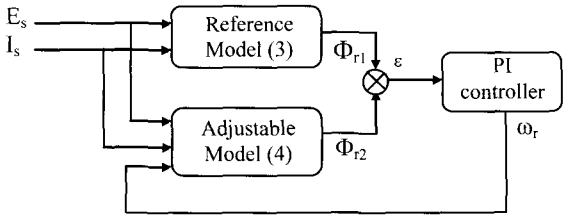

Fig. 4. MRAS-based Speed estimator

Where: $w_1 = \left(1 - \frac{T_s}{T_r}\right)$ $w_2 = T_s\omega_r$ $w_3 = \frac{T_s L_m}{T_r}$

This model is a simple two-layer neural network where w_1, w_2 and w_3 represent the weights. The inputs [k-1] can be obtained from the outputs [k] by a simple time delay z^{-1}. However to avoid instability, the rotor flux input signal are those coming from the output of the voltage model and not from the ANN model [8]. So, the delayed outputs of the voltage model are used as inputs to the neural network. This modification implies a faster and more stable convergence of the estimator.

The weights are adjusted so as to minimize a square error energy function and the new weight w_i is given by:

$$w_i[k] = w_i[k-1] + \eta\Delta w_i[k] + \alpha\Delta w_i[k-1] \quad (7)$$

Where η is the training coefficient and α determines the effect of the past weight changes on the current weight. The dynamic convergence of the ANN depends on the choice of η and α. The higher learning rate η causes bigger ripples in estimated speed but achieves a fast response of estimator. However, the dynamic behavior in the smaller learning rate η is lower. We choose a learning coefficient that is as large as possible without leading to more oscillations. This offers the most rapid learning and hence the estimated speed tracks the real speed in good agreement. Therefore, the speed can be calculated by dividing w_2 by the sampling period Ts [13]. The bloc diagram of the ANN speed estimator is shown in Fig. 5.

4. Experimental Results

The vector control and the speed estimation have been implemented in C language with the use DS1104 DSP Board. For control superpose, the induction machine is modeled by a set of equations (1) related to Fig. 1 and a modified vector controller is used to compensate saturation and iron loss effects (Fig.2) [9-10]. The estimated speed has been feedback and used both for the speed regulation and the orientation angle computation. While the actual speed is used only to compute the speed error (Fig. 6 and Fig. 7).

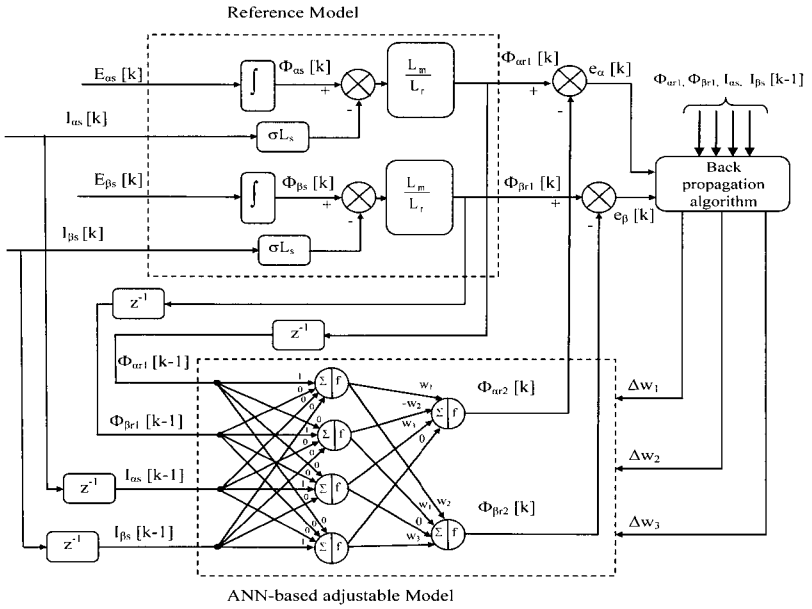

Fig. 5. Artificial Neural Network-based Speed estimator

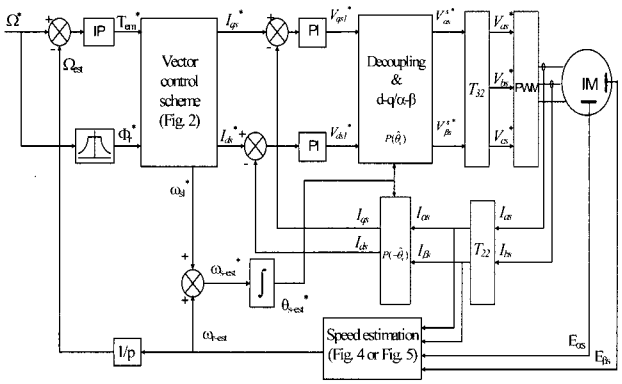

Fig. 6. Sensorless vector control block diagram

Fig. 7. Experimental setup

Fig.8 presents the experimental results obtained for speed inverting from -480 rpm to 480 rpm. Estimated speed, actual speed, reference speed and error in speed are shown in this figure. It can be seen that the estimated speed tracks the actual speed very well and the speed reversal is accomplished in less than 0.5s and the performance of the sensorless control is very satisfactory. Furthermore, low speed operation is performed (Fig. 9 and Fig. 10). The speed estimation exhibits a few oscillations which may lead to halting of the system if we decrease more the speed. The speed estimation can not be improved regarding to the difficult of e.m.f measurement in low speed rang, the noise has a negative influence in this operation domain, it affects the fundamental e.m.f signal. However, the four quadrant operation is still possible, the speed response is very quick and it converges to the reference value (Fig. 11). Hence, the sensorless vector control, where low speed operation is required, is a very sensitive task.

The load application is then verified (Fig.12), the drive operates at 860 rpm reference speed and a constant torque of 60% of rated torque is applied at t=1s. It is clear that the drive response occurs immediately when torque step is given. The estimated speed tracks the actual speed while in transients. However, a little static speed error appears with the ANN-based MRAS speed estimator. These results demonstrate also that classical MRAS and ANN estimators, in nominal operation, have globally the same behavior.

The speed estimator model uses electrical parameters of the induction motor, Hence, incorrect parameters in speed estimator lead to an estimate speed error. Fig. 13 shows the experimental results of the sensorless vector control drive when speed is increased via a ramp from 860 to 1720 rpm. The value of the mutual inductance used in the MRAS and the ANN speed estimators is set to the constant nominal value. The comparison between MRAS and ANN-based estimators leads to the positive appreciation of the latter.

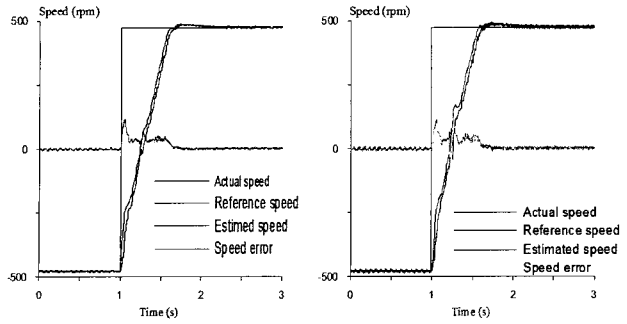

(a) MRAS speed estimator (b) ANN speed estimator

Fig. 8. Speed reversal from -480 to 480 rpm

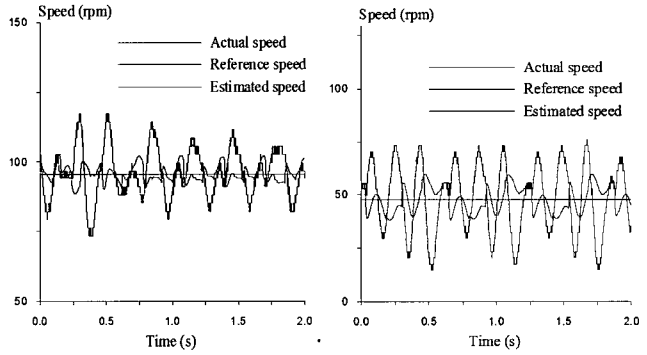

(a) 95 rpm (b) 48 rpm

Fig. 9. Low speed operation by using MRAS speed estimator

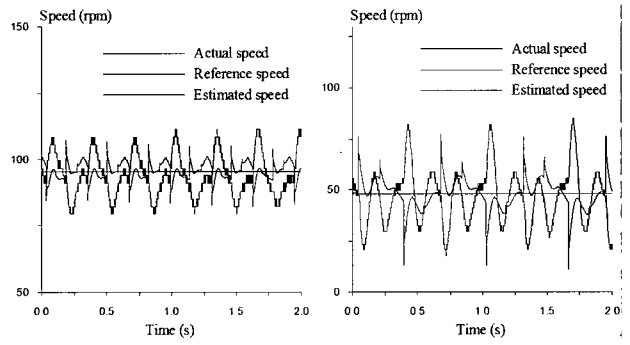

(a) 95 rpm (b) 48 rpm

Fig. 10. Low speed operation by using ANN speed estimator

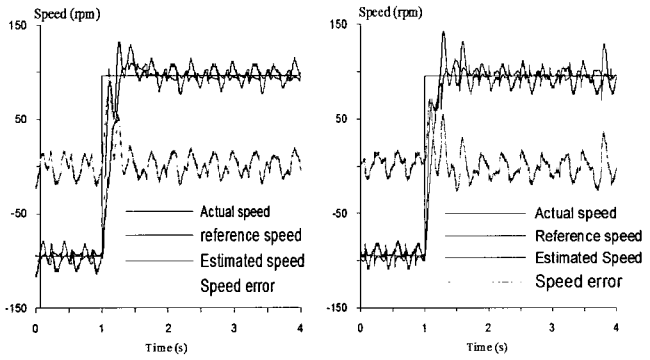

(a)MRAS speed estimator (b) ANN speed estimator

Fig. 11. Speed reversal from -95 to 95 rpm

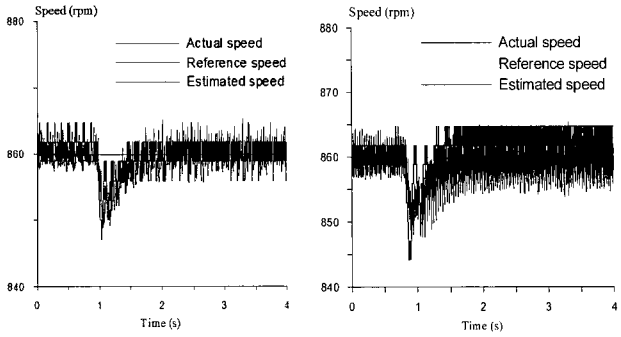

(a) MRAS speed estimator (b) ANN speed estimator

Fig. 12. Load application

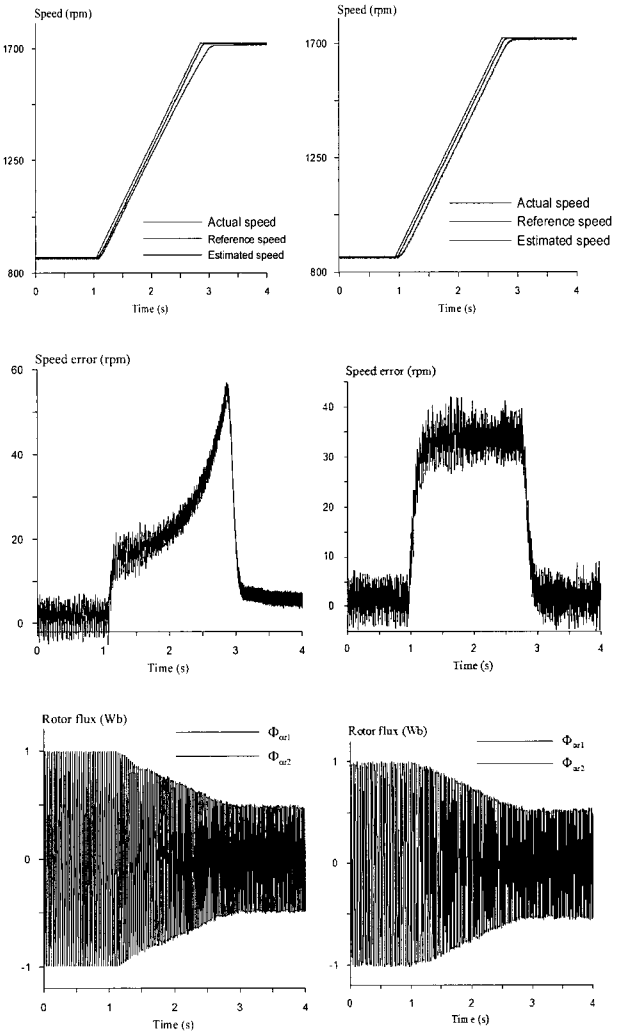

(a) MRAS speed estimator (b) ANN speed estimator

Fig.13. High speed operation with flux weakening

With MRAS-based speed estimator the estimated speed is lower than the actual speed in the weakening region and a steady state static error of 8 rpm occurs due to the variation of the mutual inductance that is neglected in speed estimator. The reason is that the stator flux estimated by the current model is different from that estimated from

voltage model because this last contains the L_r/L_m ratio that does not change (L_r and L_m vary in the same order). However, the adjustable model needs $1/T_r$ ratio that is greatly affected by the saturation effect.

With the ANN-based speed estimator, the estimated speed coincides with the actual speed exactly and the main speed error is essentially eliminated. The input rotor flux of the adjustable model is the output rotor flux of the reference model that is not affected by saturation effect. In addition, the adjustable model contains the weights w_1, w_2 and w_3 that are adjusted on line and at each sampling period. So, in the ANN-based MRAS speed estimator, the parameter variation effect is eliminated. And the speed control performance is improved by substituting the MRAS by an ANN speed estimator in the flux weakening operation.

5. Conclusion

Modified flux integration method, based on e.m.f measurement, is integrated in speed estimation. MRAS-based and ANN-based speed estimation algorithms of an induction motor were proposed. From the experimental results, it is shown that the proposed algorithms estimate the speed exactly in nominal speed and the dynamic performances are very satisfactory. But in a low speed range, oscillations of the speed occurred; the oscillations are due to the difficulty to measure a no-noise e.m.f. These estimators also have a robust speed estimation performance even with load variation or variable-speed operation. Finally, the performance of MRAS speed estimation in the field weakening region was deteriorated due to the saturation level variation. However, in the ANN speed estimation, the estimated speed follows the actual speed and the error included in the estimated speed was removed.

Appendix (Induction machine data)

P_n = 5.5 KW U_n = 380V P = 2
R_s = 2.25 Ω R_r = 0.7 Ω R_{Fe} = 480 Ω
L_{mN}=112 mH $L_{\sigma s}$ = 11.4 mH $L_{\sigma r}$ = 0.4 mH
$T_{em\,n}$ = 35 N.m J=0.06093 kgm^2

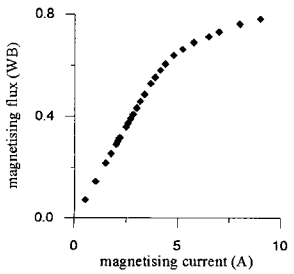

Fig.a1: Magnetizing flux versus magnetizing current

References

[1] I. Boldea, S. A. Nasar, "Unified treatment of core losses and saturation in orthogonal axis models of electric machines", *Proc. IEE*, vol. 134, pt. B, pp. 353-363, 1987.

[2] P. Vas, "Generalized transient analysis of saturated a-c machines", *Archiv für Electrotechnik*, vol. 63, pp. 57-62, 1981.

[3] E. Levi, M. Sokola, A. Boglietti, M. Pastorelli, "Iron loss in rotor flux oriented induction machines: Identification, Assessment of detuning and compensation", *IEEE, Trans. on Power Electronics*, vol. 11, no. 5, pp. 698-708, Sept. 1996.

[4] S. Moulahoum, O. Touhami, "Generalized approach to an induction machine modeling in presence of saturation and iron loss", in *Proc. 2005 IEEE, annual meeting of Power Engineering Society PES'05*, pp. 478-482, Juin 2005.

[5] J. Jung, K. Nam "A vector control scheme for EV induction motors with a series iron loss model", *IEEE, Trans. on Industrial Electronics*, vol. 45, no. 4, pp. 617-624, August 1998.

[6] L. Baghli, H. Razik, A. Rezzoug, "A stator flux oriented drive for an induction motor with extra (α,β) coils", in *Proc. 1998 IEEE Industrial Electronics Conf. IECON'98*, vol. 4, pp. 2522-2526, Sept. 1998.

[7] E. Levi, M. Wang, "A speed estimator for high performance sensorless control of induction motors in the field weakening region", *IEEE Trans. on Power Electronics*, vol. 17, no. 3, pp. 365-378, May 2002.

[8] M. Cirrincione, M. Pucci, G. Cirrincioni, G. A. Capolino, "A new TLS based MRAS speed estimation with adaptative integration for high performance induction machine drives", *IEEE Trans. on Industry Applications*, vol. 40, no. 4, pp. 1116-1137, July 2004.

[9] O. Touhami, R. Ibtiouen, S. Moulahoum, S. Mekhtoub, "Analysis and compensation of parameters effect in vector controlled induction machine", *Archives of Electrical Engineering*, vol. 50, no. 2, pp.165-182, April 2001.

[10] S. Moulahoum, O. Touhami, A. Rezzoug, L. Baghli, "Vector controlled induction machine by considering series iron losses equivalent circuit and magnetic saturation", *WSAES, Transactions on Systems*, vol. 4, no. 11, pp. 1861-1869, Nov. 2005.

[11] L. Ben-brahim, S. TadaKuma, A. Akdag, "Speed control of induction motor without rotational transducers", *IEEE Trans. on Industry Applications*, vol. 35, no. 4, pp. 844-849, July 1999.

[12] C. Schauder, "Adaptive speed identification for vector control of induction Motors without rotational

transducers", *IEEE, Trans. on Industry Applications*, vol. 28, no. 5, Sept. 1992.

[13]S. Moulahoum, O. Touhami, "Modified sensorless field oriented control of induction machine", in *Proc. 2006 IEEE, 17th Inter. Conf. on Electrical Machines, ICEM 2006*, Chania, Greece, Sept. 2006.

Samir Moulahoum was born in Algiers in 1971. He received the Engineer degree in Electrical Machines in 1995 and the Magister degree in Electrical Engineering in 1998 and the Doctorate degree in Power Elctronics and Drives in 2006 from University of Sciences and Technology of Algiers USTHB. He was with GREEN laboratory, UHP University, Nancy, France, as invited researcher for two years. He worked in the National Electricity and Gas Company as studies engineer for two years. He is actually an assistant professor in Electrical Department at Médéa University Center. His research interests are Electric Machines, Power Electronics, Control of Electrical Drives and DSP Implementation.

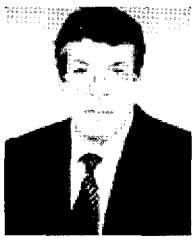

Omar Touhami received the Engineer, Master and Doctorate degrees in Electrical Engineering in 1981, 1986 and 1994 respectively from National Polytechnic School of Algiers. He is currently a professor in Electrical Engineering Department at National Polytechnic School of Algiers. His research interests have including Electric Machines, Variable Speed Drives, and Power Systems. From 1989 to 1994, he was associater esearcher in the Research Center in Automatic of Nancy (CRAN-ENSEM-INPL) where his works in identification of electric machines received a success by the industrial. He is actually reviewer in IEEE Transaction On Energy Conversion. He is also Director of Research Laboratory in National Polytechnic School of Algiers since 2000 on 2005.